

FilterViT and DropoutViT

1st Bohang Sun

*School of Information and Software Engineering
University of Electronic Science and Technology of China
Chengdu, China
bobsun@std.uestc.edu.cn*

Abstract—In this study, we propose an improved variant of MobileViT that performs attention-based QKV operations in the early stages of downsampling. Directly conducting QKV operations on high-resolution feature maps is computationally intensive due to the large size and numerous tokens. To address this issue, we introduce a filter attention mechanism using a convolutional neural network (CNN) to generate an importance mask (Filter Mask) that selects the most informative pixels for attention computation.

Specifically, the CNN scores the pixels of the feature map, and we sort these scores to select the top K pixels (with K varying across network layers). This method effectively reduces the number of tokens involved in the attention computation, thereby lowering computational complexity and increasing processing speed. Additionally, we find that the importance mask offers interpretability, as the model focuses more on regions of the image that are crucial to the outcome.

Experimental results demonstrate that our model achieves advantages in parameter efficiency and computational speed while improving accuracy. Compared to other models, our approach significantly reduces computational resource consumption while maintaining high performance.

Index Terms—MobileViT, Transformer, Efficient Attention, Learned Sparse Attention, Convolution, Interpretability

I. INTRODUCTION

Vision Transformer (ViT) [1] has revolutionized the field of computer vision by introducing transformer-based architectures to image tasks. ViT leverages attention mechanisms over 16×16 image patches, allowing for global context learning across the image. However, while ViT achieves state-of-the-art results on various tasks, its reliance on large tokens makes it computationally expensive when applied to high-resolution images. The quadratic complexity of the QKV operation [2] means that increasing the number of tokens dramatically increases the computational burden.

To address this issue, MobileViT [3] was introduced as a lighter version of ViT, which performs attention after downsampling the image. This reduces the number of tokens involved in attention, thus improving computational efficiency. However, MobileViT sacrifices granularity by operating on downsampled feature maps (e.g., 56×56 or 28×28), which may limit its ability to capture finer details. Moreover, not all pixels contribute equally to the final prediction. Many pixels are noisy or irrelevant, while others are critical for decision-making.

In this paper, we propose a new variant of MobileViT, called **FilterViT**, that allows for more granular attention without the

need for early downsampling. Our approach leverages a convolutional neural network (CNN) to generate an importance mask, which determines which pixels in the feature map are most relevant for attention. By sorting the pixel importance scores and selecting the top K pixels, we perform attention on only the most significant parts of the image, thereby reducing the computational complexity of the QKV operation.

Unlike the challenging task of implementing sparse matrix operations on GPUs, our method offers a practical solution by selecting important pixels directly. This ensures that the computational load is reduced while maintaining accuracy. Additionally, our approach offers interpretability, as the importance mask highlights the critical areas of the image that the model focuses on during attention. For example, in an image of a lamb, the mask effectively highlights the contour of the lamb while ignoring irrelevant background features.

In summary, our contributions are threefold:

- We introduce a lightweight, more efficient attention mechanism that allows for finer-grained attention while reducing computational complexity.
- Our method inherently provides interpretability by focusing attention on the most relevant regions of the image, as demonstrated through visualizations of the importance mask.
- Through an ablation study, we introduce **DropoutViT**, a variation of our model that mimics dropout by randomly selecting pixels, further validating the flexibility and robustness of our approach.

II. RELATED WORK

A. Vision Transformers

Vision Transformers (ViT) [1] have demonstrated significant success in computer vision tasks by applying attention mechanisms to image patches, typically 16×16 patches. While ViT excels at capturing global dependencies across the image, the quadratic complexity of its QKV operations [2] poses a computational challenge, particularly for high-resolution images. The number of tokens increases rapidly, leading to significantly higher computational costs as the image resolution grows.

B. MobileViT

MobileViT [3] addresses this issue by downsampling the image before applying transformer-based attention. By performing attention at smaller resolutions (e.g., 56×56 or 28×28),

it reduces the number of tokens and thus lowers computational complexity. However, this downsampling sacrifices the granularity of attention, as finer details may be missed when attention is applied to a lower-resolution feature map.

C. Efficient Attention Mechanisms

Several attention-based models have been proposed to optimize computational complexity. Longformer [4] employs a sparse attention mechanism, restricting attention to a local window around each token, which reduces the computational load but may struggle to capture global dependencies in images. Performer [5] approximates softmax attention using kernel-based methods, achieving linear complexity with respect to sequence length, a promising approach for reducing the cost of attention in vision tasks. Linformer [6] further reduces complexity by projecting keys and values into lower dimensions, maintaining linear complexity while conserving memory. Reformer [7] introduces locality-sensitive hashing (LSH) to approximate nearest neighbors in attention space, making the computation more efficient, though this approach may face challenges when highly detailed structures require attention.

D. Lightweight Convolutional Architectures

In addition to attention mechanisms, lightweight convolutional architectures have been developed to balance efficiency and performance. MobileNetV2 [8] introduces an inverted residual block to optimize information flow with fewer parameters. MobileNetV3 [9] improves on this by using neural architecture search (NAS) to design an efficient structure, optimizing both latency and accuracy. EfficientNet [10] scales networks by balancing depth, width, and resolution, achieving optimal performance across configurations. GhostNet [11] reduces feature map redundancy by generating fewer feature maps, thus improving speed and reducing parameter count. Finally, LCNet [12] focuses on low-complexity convolutional operations to achieve faster inference times while maintaining reasonable accuracy, making it ideal for edge computing tasks.

E. Filter Attention Mechanism

Our work builds upon these advancements by introducing the Filter Attention mechanism. Unlike models that downsample or linearize attention computations, our approach selectively applies attention to the most important pixels using a CNN-generated filter mask. By sorting the pixels based on their importance and selecting the top K pixels, we reduce the number of tokens involved in the QKV computation. This maintains global context while significantly reducing computational complexity, without sacrificing attention granularity. Our approach also offers interpretability, as visualizing the filter mask shows that the model effectively focuses on the most relevant parts of the image.

III. METHOD

A. Structure

In our proposed network architecture, we combine convolutional layers with transformer layers to balance local feature

extraction and global attention. The key innovation of our method is the introduction of a Filter Attention mechanism, which selectively attends to important regions of the feature map, significantly reducing the computational complexity of attention-based operations.

The network processes the input image through a CNN, which produces a feature map. This feature map is treated as a set of tokens that are reshaped and passed through a Transformer Encoder [2]. Unlike traditional attention mechanisms, our Filter Attention selectively identifies important tokens based on a filter mask generated by the CNN, which is applied to reduce the number of tokens used in the attention computation. This mechanism allows the model to ignore irrelevant regions of the image, as not every pixel contributes equally to the final prediction. In theory, some pixels may represent noise or unnecessary details, and even among useful pixels, their contributions to the prediction are not uniform [13].

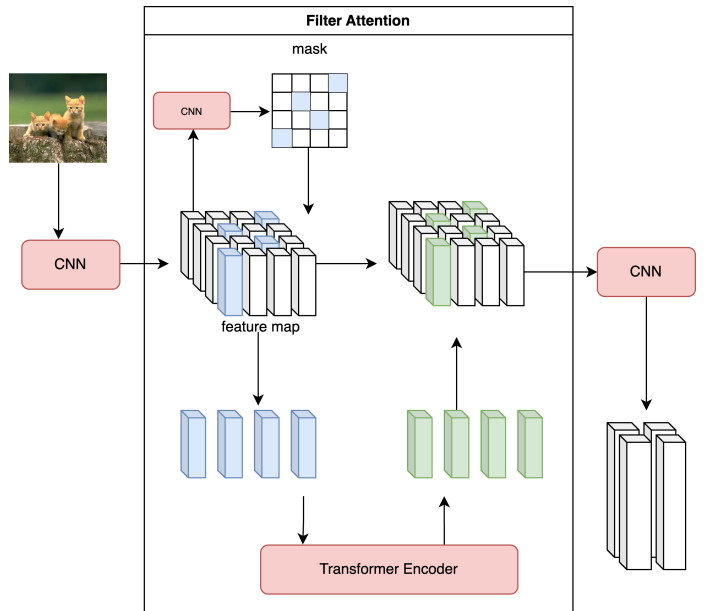


Fig. 1: An overview of the Filter Attention mechanism. The input image is first processed by a convolutional neural network (CNN) to generate a feature map. A filter mask is then applied to this feature map, which selects the most important pixels for further attention-based computation. Only the top-ranked pixels, based on the importance scores, are passed through the Transformer Encoder for global attention processing. This reduces the computational complexity by focusing attention on the most relevant regions of the image.

B. Filter Attention Block

The core of our method is the Filter Attention block, which integrates a convolutional block with a transformer encoder. The key idea is to treat the pixels in the feature map as tokens for the transformer encoder, but instead of processing all tokens, we apply a filter mask to select only the most important ones.

Initially, an image is processed through a CNN module, generating a feature map denoted as X_f , where $X_f \in \mathbb{R}^{N \times C \times H \times W}$. The CNN also produces a filter mask, denoted as $M \in \mathbb{R}^{N \times 1 \times H \times W}$, which assigns importance scores to each pixel. The feature map is then element-wise multiplied by the mask to filter out less important tokens, as expressed by the formula:

$$X_{filtered} = X_f \odot M$$

Here, \odot denotes element-wise multiplication, which ensures that only the most relevant pixels are preserved for further attention-based computation.

Next, $X_{filtered}$ is reshaped into a transformer-compatible shape X_t , where $X_t \in \mathbb{R}^{N \times C \times K}$, with K being the number of selected tokens after filtering. The filtered tokens are passed through a Transformer Encoder [2], producing the output X'_t .

The FilterAttention mechanism is detailed in Algorithm 1. It selectively focuses on the most informative pixels in the feature map by computing an importance map and applying a Transformer Encoder to the selected pixels. This approach significantly reduces computational complexity while retaining critical spatial information.

Algorithm 1 FilterAttention Mechanism

Require: Feature map $x \in \mathbb{R}^{B \times C \times H \times W}$

- 1: Compute importance map: $\text{imp} = \sigma(\text{Conv}(x))$
- 2: Select top K indices per sample: $\text{indices} = \text{TopK}(\text{imp}, K)$

- 3: Mask feature map: $x \leftarrow x \odot \text{imp}$
- 4: Extract selected pixels and add positional encoding:

$$\text{sel_pixels}[b, k] = x[b, :, i, j] + \text{pos}[i \times W + j]$$

where $(b, i, j) \in \text{indices}$

- 5: Apply Transformer Encoder:

$$\text{tokens} = \text{TransformerEncoder}(\text{sel_pixels})$$

- 6: Update feature map at selected indices:

$$x[b, :, i, j] \leftarrow \text{tokens}[b, k]$$

where $(b, i, j) \in \text{indices}$

- 7: **return** Updated feature map x
-

C. Inverted Residual Block

In our network, we employ the Inverted Residual Block [8] to enhance feature extraction while maintaining model efficiency. This block is designed to first expand the input channels, apply depthwise convolution, and then project the output back to the original dimensions, creating a residual connection. This structure ensures that important spatial information is preserved while reducing the number of parameters in the model, making it computationally efficient for both small and large-scale vision tasks.

D. Global Self-Attention with Pooling

To further reduce the computational complexity of the attention mechanism, we apply average pooling to the feature map before feeding it into the self-attention layers. Pooling reduces the spatial dimensions of the input feature map, which lowers the number of tokens passed into the attention module, thereby decreasing the quadratic cost of QKV operations. Despite this reduction, global context is maintained, ensuring that the model can still capture long-range dependencies between the most relevant regions of the image.

E. Transformer Encoder

The selected tokens from the filtered feature map are processed through the Transformer Encoder [2]. The transformer layer applies self-attention to capture global dependencies between tokens. After passing through the transformer, the tokens are reshaped back into their original spatial dimensions and processed through subsequent CNN layers for further refinement.

Finally, the output feature map is used for classification or other downstream tasks, leveraging both local and global information extracted from the image.

IV. EXPERIMENT

We conducted experiments using five distinct img-100 subsets, each randomly sampled from the ImageNet-1K dataset [14]. The results presented in this paper are based on the first img-100 subset. To ensure a fair comparison, the same training settings and hyperparameters were applied uniformly across all models. The specific class selections for the five img-100 subsets used in this study are provided on GitHub for reference and reproducibility at the following address: <https://github.com/BobSun98/FilterViT>.

A. Dataset

The img-100 subsets were constructed from 100 randomly selected classes within the ImageNet-1K dataset [14]. Training and validation were performed on these subsets. Each model was trained on five distinct subsets to enhance robustness and reduce overfitting, ensuring that the reported results are not skewed by the selection of a particular subset. The smaller img-100 dataset allows for faster prototyping and algorithm validation, while still posing a challenge in reducing overfitting. If lightweight models perform well on a smaller dataset, it indicates their potential for better generalization.

1) *Data Augmentation:* To improve the generalization ability of all models, we applied consistent data augmentation techniques during training. These techniques included RandomResizedCrop(224) to randomly crop and resize images to 224×224 pixels, RandomHorizontalFlip to randomly flip images horizontally, TrivialAugmentWide [15] to introduce broad augmentation variability, and Normalization with a mean of [0.5, 0.5, 0.5] and a standard deviation of [0.5, 0.5, 0.5]. During validation, images were resized to 256×256 pixels, followed by a center crop to 224×224 pixels, with normalization applied using the same mean and standard deviation values.

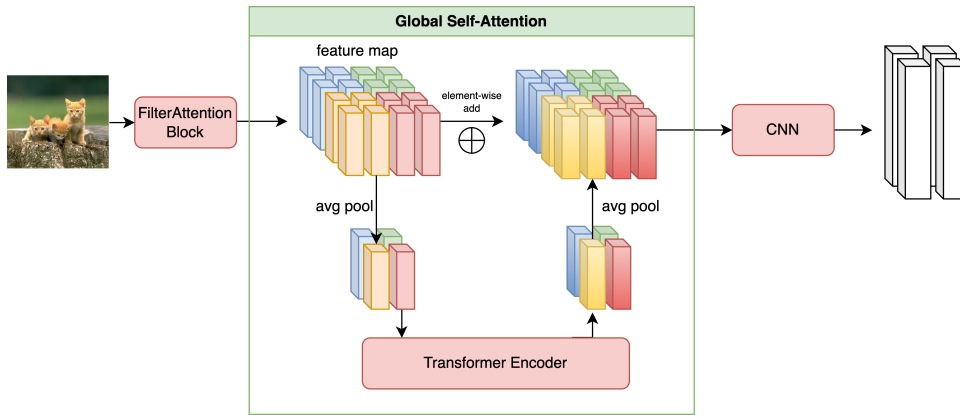


Fig. 2: Illustration of the Global Self-Attention mechanism with pooling. After the initial feature extraction by the CNN, average pooling is applied to reduce the size of the feature map. This pooling operation significantly decreases the number of tokens passed into the Transformer Encoder for self-attention computation. The remaining tokens retain global context and are processed by the self-attention module, capturing long-range dependencies in the image with reduced computational cost.

B. Training and Hyperparameters

All models were trained using the same hyperparameters. The batch size was set to 64, with a learning rate of 0.0005, which was decayed using a cosine annealing schedule [16] to a minimum learning rate of $1e-5$. The models were trained for 120 epochs using the AdamW optimizer [17], where β_1 was set to 0.9, β_2 to 0.999, and the weight decay was 0.01. The learning rate scheduler, CosineAnnealingLR, had a T_{\max} of 120 epochs, with a minimum learning rate of $1e-5$.

C. Hardware Configuration

Training was conducted on a Tesla P40 GPU. Performance in terms of frames per second (FPS) for CUDA was measured on an RTX 4090 GPU, while CPU performance was evaluated on an Apple M1 Pro chip. These hardware configurations allow for a comparison of each model’s efficiency across both high-performance and resource-constrained environments.

V. EXPERIMENT

We conducted experiments using five distinct img-100 subsets, each randomly sampled from the ImageNet-1K dataset [14]. The results presented in this paper are based on the first img-100 subset. To ensure a fair comparison, the same training settings and hyperparameters were applied uniformly across all models. The specific class selections for the five img-100 subsets used in this study are provided on GitHub for reference and reproducibility at the following address: <https://github.com/BobSun98/FilterViT>.

A. Dataset

The img-100 subsets were constructed from 100 randomly selected classes within the ImageNet-1K dataset [14]. Training and validation were performed on these subsets. Each model was trained on five distinct subsets to enhance robustness and reduce overfitting, ensuring that the reported results are not skewed by the selection of a particular subset. The smaller img-100 dataset allows for faster prototyping and algorithm

validation while still posing a challenge in reducing overfitting. If lightweight models perform well on a smaller dataset, it indicates their potential for better generalization.

1) *Data Augmentation*: To improve the generalization ability of all models, we applied consistent data augmentation techniques during training. These techniques included RandomResizedCrop(224) to randomly crop and resize images to 224×224 pixels, RandomHorizontalFlip to randomly flip images horizontally, TrivialAugmentWide [15] to introduce broad augmentation variability, and normalization with a mean of $[0.5, 0.5, 0.5]$ and a standard deviation of $[0.5, 0.5, 0.5]$. During validation, images were resized to 256×256 pixels, followed by a center crop to 224×224 pixels, with normalization applied using the same mean and standard deviation values.

B. Models and Baselines

To evaluate the effectiveness of our proposed **FilterMobileViT**, we compared it against several baseline models that represent a range of architectures in the field of efficient neural networks. These include **MobileNetV2** [8], known for its inverted residual blocks and linear bottlenecks, and **MobileNetV3** [9], which improves upon its predecessor with neural architecture search and hard-swish activation functions. We also included **EfficientNet-Lite0** [10], which balances network depth, width, and resolution for optimal efficiency, and **GhostNet** [11], which reduces redundancy in feature maps to improve computational performance.

In addition to convolutional architectures, we compared against lightweight transformer-based models such as **TinyViT** [18], a compact vision transformer designed for high performance with fewer parameters, and **LeViT** [19], a hybrid model that combines convolutional and transformer layers for efficient inference. We also included **TinyNet** [20], a family of models optimized for small parameter sizes and computational costs, and **LCNet** [12], which prioritizes speed in its lightweight convolutional network design. Finally, **MobileViT**

S [3] was included as it incorporates transformer layers into a mobile-friendly architecture, similar to our approach.

These models were selected to provide a comprehensive comparison across different architectural strategies, highlighting the strengths of our **FilterMobileViT** in terms of accuracy and efficiency.

C. Training Details

All models were trained with consistent hyperparameters: a batch size of 64 and the AdamW optimizer [17] ($\beta_1 = 0.9$, $\beta_2 = 0.999$, and a weight decay of 0.01). The initial learning rate was set to 0.0005 and decayed following a cosine annealing schedule [16] to a minimum of 1×10^{-5} , over 120 epochs. CosineAnnealingLR was used as the learning rate scheduler, with $T_{\max} = 120$ epochs. Training was performed on a Tesla P40 GPU, while inference performance was measured on both an RTX 4090 GPU for CUDA and an Apple M1 Pro chip for CPU. These configurations allowed for a comprehensive comparison of model efficiency across different hardware environments, ranging from high-performance GPUs to resource-constrained CPUs.

D. Experimental Results

As shown in Table I, **FilterMobileViT** achieves a strong balance between accuracy and computational efficiency. With only 1.89 million parameters, it achieves an accuracy of 0.861, outperforming most other models except for **Tiny-ViT** [18], which achieves a slightly higher accuracy of 0.876 but with significantly more parameters (10.59M). This indicates that while Tiny-ViT offers marginally better performance, FilterMobileViT provides a more efficient solution in terms of model size, making it more suitable for deployment in resource-constrained environments.

FilterMobileViT also demonstrates competitive performance in terms of frames per second (FPS). Although it falls slightly behind models like **LCNet_100**, which achieves higher FPS on both CPU and CUDA platforms, LCNet prioritizes speed over accuracy, resulting in a lower accuracy of 0.808. In contrast, FilterMobileViT offers a better trade-off between speed and accuracy, maintaining high accuracy with reasonable computational efficiency.

Moreover, compared to other lightweight models such as **MobileNetV2** [8] and **GhostNet** [11], FilterMobileViT not only reduces the parameter count but also enhances accuracy. For instance, MobileNetV2 has 2.35 million parameters with an accuracy of 0.833, while GhostNet has 4.02 million parameters and achieves an accuracy of 0.842. This improvement underscores the effectiveness of our Filter Attention mechanism in selectively focusing on the most informative regions of the image, leading to better performance without increasing computational costs.

In terms of inference speed, while **EfficientNet_Lite0** and **MobileNetV3_Small** offer higher FPS on CUDA, they suffer from lower accuracy compared to FilterMobileViT. This further highlights the advantage of our approach in achieving a

balanced performance suitable for practical applications where both accuracy and efficiency are critical.

Overall, FilterMobileViT demonstrates that incorporating the Filter Attention mechanism can lead to significant improvements in accuracy and efficiency, outperforming several established models in the field. Its lower parameter count and competitive speed make it an attractive option for deployment on devices with limited computational resources.

E. Accuracy and Loss Curves

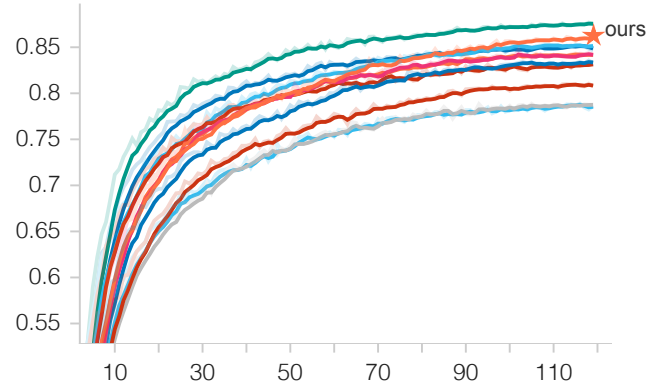


Fig. 3: Validation accuracy over epochs for the first img-100 subset.

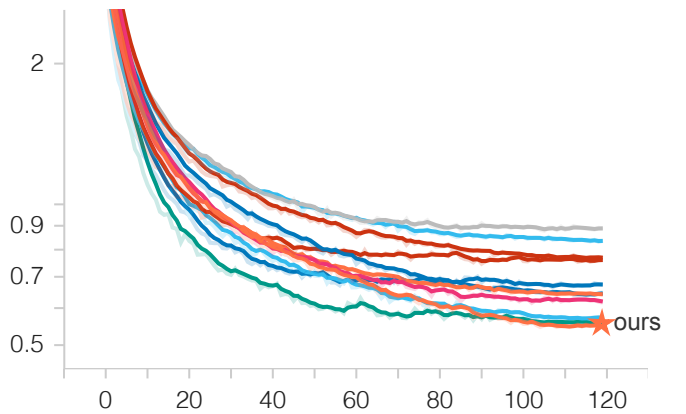


Fig. 4: Validation loss over epochs for the first img-100 subset.

Figures 3 and 4 show the validation accuracy and loss curves for the first img-100 subset. As depicted in the accuracy curve, FilterMobileViT converges rapidly and maintains competitive accuracy throughout the training process, closely approaching Tiny-ViT’s performance while maintaining a much smaller parameter count. The loss curve similarly demonstrates that FilterMobileViT achieves stable convergence with minimal overfitting. The results for the other four img-100 subsets can be found in the Appendix.

SELF-EXPLAINABILITY

Previous research has aimed to explain and visualize the behavior of vision models and Vision Transformers (ViT).

TABLE I: Comparison of Models on the First Subset

Model	#Params (M)	FPS (CPU)	FPS (CUDA)	Accuracy
MobileNetV2_100	2.35	11.29	848	0.833
MobileNetV3_Large_100	4.33	6.57	742	0.832
MobileNetV3_Small_100	1.62	7.14	892	0.786
EfficientNet_Lite0	3.49	3.63	873	0.841
Tiny-ViT-11M-224	10.59	6.19	524	0.876
LeViT_128	8.52	12.96	442	0.787
GhostNet_100	4.02	8.60	464	0.842
TinyNet_A	5.03	2.75	475	0.848
LCNet_100	1.80	7.29	1377	0.808
MobileViT_S	5.00	6.14	485	0.851
FilterMobileViT (ours)	1.89	5.60	410	0.861

For instance, [21] introduced the Attention Rollout method to visualize attention maps, providing insights into where the model focuses during prediction. Similarly, [22] developed techniques to analyze the internal representations of ViTs by clustering their learned features. Furthermore, Vit-CX [13] leverages representations from the last layer of ViTs and employs clustering to represent the model’s focus areas. In our experiments, we found that FilterViT inherently possesses interpretability without the need for additional visualization techniques.

To better understand the behavior of FilterMobileViT, we visualized the filter masks generated by each Filter Attention layer. This was done by running inference on a set of test images from a pre-trained model and extracting the filter masks at different layers. These masks were then resized to match the original image dimensions and overlaid on the input images to provide a clear visual representation of where the model is focusing its attention [23].

In the first Filter Attention layer, the model tends to focus on both the foreground and background, sometimes highlighting object edges. This suggests that the first layer is responsible for identifying broad and general features across the image. As we move deeper into the second layer, the focus shifts more towards the main object or foreground of the image, indicating that the model has started to refine its attention and concentrate on the most salient features. In the third and final layer, the attention shifts back to the background, possibly to refine the overall context and ensure that irrelevant regions are appropriately weighted.

This collaborative behavior between the layers demonstrates that the Filter Attention mechanism not only selects important regions for computation but also helps the model understand the image at different granularities. By progressively refining its attention from edges to the main object and then to the background, FilterMobileViT exhibits explainability in its decision-making process, which can be visualized as seen in Fig. 5.

These observations highlight that the model’s filter masks are not arbitrary but rather reflect a structured approach to understanding the image. Each layer contributes a distinct aspect of the image, allowing the model to efficiently balance attention between foreground objects and the broader context. This layered attention structure not only improves performance but also provides a more interpretable understanding of how

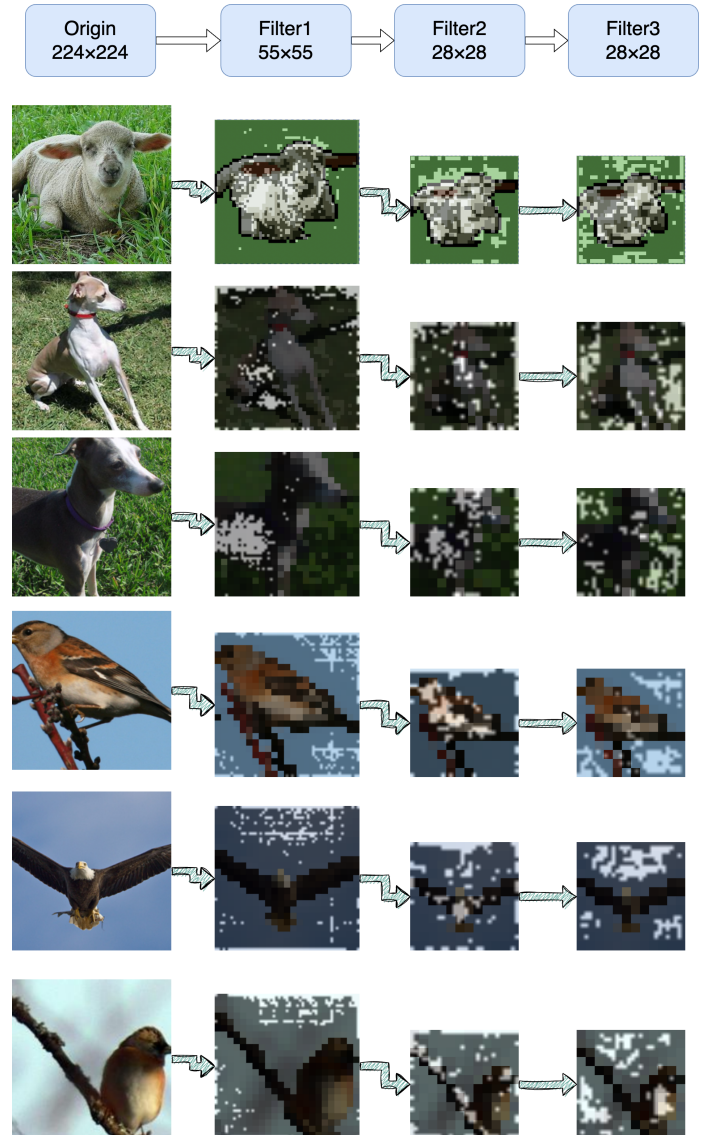


Fig. 5: Visualization of filter masks across three Filter Attention layers. The first layer focuses on edges and general features, the second on the main object, and the third on the background. This layered attention mechanism suggests that FilterMobileViT has inherent explainability.

the model processes visual information, simultaneously validating the correctness of the design.

ABLATION STUDY: DROPOUTVIT

In this study, we introduced a variant of our FilterViT model called DropOutViT. The key difference between DropOutViT and FilterViT lies in how the model selects pixels for attention computation. While FilterViT utilizes a CNN-generated filter mask to deterministically select the most important pixels, DropOutViT replaces this mechanism with a random sampling approach, where a subset of pixels is randomly selected to pass through the Transformer Encoder during each training step. This can be considered analogous to applying dropout in the attention computation, introducing a degree of stochasticity into the selection process [24].

The rationale behind DropOutViT is to explore whether random sampling of pixels could lead to similar or improved performance by preventing overfitting to specific features. By introducing randomness, we hypothesize that the model may generalize better, especially during the early training stages when the filter mask in FilterViT is not yet fully optimized.

1) *DropOutViT vs. FilterViT*: We compared the performance of DropOutViT and FilterViT across several training runs (see Fig. 6). Initially, both models exhibited similar performance, with DropOutViT even outperforming FilterViT slightly during the early epochs. This may be attributed to the increased diversity in the features selected by the random sampling process, which potentially prevents early overfitting.

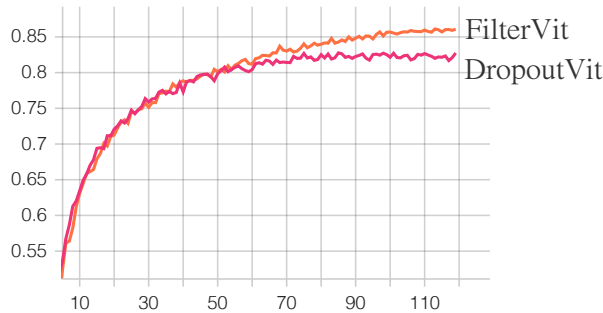


Fig. 6: Validation accuracy comparison between DropOutViT and FilterViT over the course of training.

However, as training progressed, DropOutViT appeared to reach a performance plateau around the 50th epoch, whereas FilterViT continued to improve. One plausible explanation for this is that the CNN in FilterViT gradually learns to generate more meaningful filter masks, which allows the model to focus on the most critical pixels for attention computation. This refined selection process likely enables FilterViT to achieve better overall performance, as the model increasingly benefits from targeted attention.

Despite its plateau, DropOutViT remains a promising variant. The random sampling approach shows potential, especially in scenarios where the deterministic nature of the filter mask may lead to overfitting or reduced generalization.

Future work could explore modifications such as adjusting the dropout ratio, experimenting with alternative sampling methods (e.g., Gaussian sampling or central sampling), or applying the dropout mask selectively to certain layers to further optimize DropOutViT’s performance.

REFERENCES

- [1] A. Dosovitskiy *et al.*, “An image is worth 16x16 words: Transformers for image recognition at scale,” arXiv preprint arXiv:2010.11929, 2020.
- [2] A. Vaswani, N. Shazeer, N. Parmar, J. Uszkoreit, L. Jones, A. N. Gomez, L. Kaiser, and I. Polosukhin, “Attention is all you need,” in *Advances in Neural Information Processing Systems (NeurIPS)*, 2017.
- [3] S. Mehta and M. Rastegari, “Mobilevit: Light-weight, general-purpose, and mobile-friendly vision transformer,” arXiv preprint arXiv:2110.02178, 2021.
- [4] I. Beltagy, M. E. Peters, and A. Cohan, “Longformer: The long-document transformer,” arXiv preprint arXiv:2004.05150, 2020.
- [5] K. Choromanski, V. Likhoshesterov, D. Dohan, X. Song, A. Gane, T. Sarlos, P. Hawkins, J. Davis, A. Mohiuddin, L. Kaiser *et al.*, “Rethinking attention with performers,” arXiv preprint arXiv:2009.14794, 2020.
- [6] S. Wang, B. Z. Li, M. Khabsa, H. Fang, and H. Ma, “Linformer: Self-attention with linear complexity,” arXiv preprint arXiv:2006.04768, 2020.
- [7] N. Kitaev, L. Kaiser, and A. Levskaya, “Reformer: The efficient transformer,” arXiv preprint arXiv:2001.04451, 2020.
- [8] M. Sandler, A. Howard, M. Zhu, A. Zhmoginov, and L.-C. Chen, “Mobilenetv2: Inverted residuals and linear bottlenecks,” in *Proceedings of the IEEE conference on computer vision and pattern recognition*, 2018, pp. 4510–4520.
- [9] A. Howard, M. Sandler, G. Chu, L.-C. Chen, B. Chen, M. Tan, W. Wang, Y. Zhu, R. Pang, V. Vasudevan *et al.*, “Searching for mobilenetv3,” in *Proceedings of the IEEE/CVF international conference on computer vision*, 2019, pp. 1314–1324.
- [10] M. Tan, “Efficientnet: Rethinking model scaling for convolutional neural networks,” arXiv preprint arXiv:1905.11946, 2019.
- [11] K. Han, Y. Wang, Q. Tian, J. Guo, C. Xu, and C. Xu, “Ghostnet: More features from cheap operations,” in *Proceedings of the IEEE/CVF conference on computer vision and pattern recognition*, 2020, pp. 1580–1589.
- [12] C. Cui, T. Gao, S. Wei, Y. Du, R. Guo, S. Dong, B. Lu, Y. Zhou, X. Lv, Q. Liu *et al.*, “Pp-lcnet: A lightweight cpu convolutional neural network,” arXiv preprint arXiv:2109.15099, 2021.
- [13] W. Xie, X.-H. Li, C. C. Cao, and N. L. Zhang, “Vit-cx: Causal explanation of vision transformers,” arXiv preprint arXiv:2211.03064, 2022.
- [14] O. Russakovsky, J. Deng, H. Su, J. Krause, S. Satheesh, S. Ma, Z. Huang, A. Karpathy, A. Khosla, M. Bernstein *et al.*, “Imagenet large scale visual recognition challenge,” *International journal of computer vision*, vol. 115, pp. 211–252, 2015.
- [15] S. G. Müller and F. Hutter, “TrivialAugment: Tuning-free yet state-of-the-art data augmentation,” in *Proceedings of the IEEE/CVF international conference on computer vision*, 2021, pp. 774–782.
- [16] I. Loshchilov and F. Hutter, “Sgdr: Stochastic gradient descent with warm restarts,” arXiv preprint arXiv:1608.03983, 2016.
- [17] I. Loshchilov, “Decoupled weight decay regularization,” arXiv preprint arXiv:1711.05101, 2017.
- [18] B. Wu, F. Xia, X. Huang, Y. Lin, H. Wang, P. Zhu, V. Sreenivas, A. Neelakantan, W. Wei, Z. Zhang *et al.*, “Tinyvit: Fast pretraining distillation for small vision transformers,” arXiv preprint arXiv:2207.10666, 2022.
- [19] B. Graham, A. El-Nouby, H. Touvron, P. Stock, A. Joulin, H. Jégou, and M. Douze, “Levit: a vision transformer in convnet’s clothing for faster inference,” in *Proceedings of the IEEE/CVF International Conference on Computer Vision*, 2021, pp. 12 259–12 269.
- [20] K. Han, Y. Wang, Q. Zhang, C. Xu, and C. Xu, “Model rubik’s cube: Twisting resolution, depth and width for tinynets,” *Advances in Neural Information Processing Systems*, vol. 33, pp. 190–202, 2020.
- [21] L. A. Hendricks, R. Hu, T. Darrell, and R. Girshick, “Attention rollout: Explaining vision transformer,” in *Proceedings of the IEEE/CVF International Conference on Computer Vision (ICCV)*, 2021.
- [22] S. Kumar, A. Srinivasan, and D. Kumar, “Visualizing and understanding vision transformers,” in *Proceedings of the IEEE/CVF International Conference on Computer Vision (ICCV)*, 2021.

- [23] R. R. Selvaraju, M. Cogswell, A. Das, R. Vedantam, D. Parikh, and D. Batra, "Grad-cam: Visual explanations from deep networks via gradient-based localization," in *Proceedings of the IEEE international conference on computer vision*, 2017, pp. 618–626.
- [24] N. Srivastava, G. Hinton, A. Krizhevsky, I. Sutskever, and R. Salakhutdinov, "Dropout: a simple way to prevent neural networks from overfitting," *The journal of machine learning research*, vol. 15, no. 1, pp. 1929–1958, 2014.

APPENDIX